

INFLUENCE OF PASS SCHEDULE DESIGN ON PROGRESSIVE DAMAGE OF COPPER WIRE DURING MULTI-PASS WIRE DRAWING PROCESS

(Conference ID: CFP/392/2017)

Floyd Banda¹, Levy Siaminwe² and Henry M. Mwenda³

¹Department of Mechanical Engineering, Copperbelt University, School of Engineering
P.O Box 21692, Kitwe, Zambia.

¹Corresponding e-mail: fbanda@cbu.ac.zm; floydbanda@yahoo.com

^{2,3}Department of Mechanical Engineering, University of Zambia, School of Engineering
P.O Box 32379, Lusaka, Zambia.

Abstract

A study of copper wire centerline and surface ductile damage during multi-pass wire drawing process using the finite element method is presented. Abaqus 6.14 Explicit packager was used to generate a 2D axisymmetric model of an electrolytic wrought copper wire which was subjected to five different area reductions (10, 12, 14, 16 and 18%). Based on an industrial setup, an eight-pass wire drawing process was modelled and by applying the Cockroft and Latham criterion for two selected nodes, cumulative ductile damage effects were evaluated at the nodes. Analysis of the models showed that the Cockroft and Latham damage criterion was met at 16% area reduction in the fourth multi-pass stage for the centerline nodes, whereas the criterion was met at 14% area reduction during the third multi-pass stage for the surface nodes. The models showed that ductile damage was highest for both nodes during the first multi-pass stage and lowest during the fourth multi-pass stage. For the centerline nodes damage initiation accelerated after the 14% area reduction, whereas for the surface nodes ductile damage accelerated after the 12% area reduction point. Micrographs on internal and surface void microstructures during the first and last multi-passes supported the damage models.

Keywords: Area Reduction, Cockroft and Latham Criterion, Central Burst, Ductile Damage

NOMENCLATURE

A_i, A_f - initial, final cross- sectional area
 d_i, d_f - initial, final wire diameter
 E - Elasticity modulus
 L_b - Die Bearing Length
 r - Area Reduction
 α - die semi-angle
 ε_o - effective strain

ε^f - fracture strain
 μ - coefficient of friction
 σ^* - maximum tensile stress
 σ_y - initial yield stress
 σ_e - effective stress
 σ_{eq} - equivalent (von Mises) stress
 σ_m - mean (hydrostatic) stress

INTRODUCTION

The annual world copper and copper alloy semis production has recorded a rise since 1980 as shown in

Figure 1. This increase in annual production is due to increased global demand of copper for expanding sectors such as building construction, electrical and electronic products, industrial machinery and equipment, transportation equipment and consumer and general products. Most notable is the advent of new copper applications which include antimicrobial copper touch surfaces, lead-free brass plumbing, high tech copper wire and heat exchangers (International Copper Study Group, 2016).

In order to manage the global demand and ready supply of copper wires and rods, high productivity and minimised or zero wastage is needed. Critical to achieving these requirements is the need for wire practitioners to take note of the several parameters at play during wire drawing.

In this paper, copper semis production through wire drawing practice is analysed. The major wire drawing process variables involving pass schedule designs are extensively analysed using an industrial scenario and finite element method.

Copper Wire Drawing

Copper wires and rods account for more than 58% of the world's first use capacity (International Copper Study Group, 2016) as shown in Figure 2. This makes the use of copper wires for various applications to be of great interest to copper metal fabricators and traders. The building construction and recent innovations in electrical and electronic products have contributed to this great usage. The copper wires, are therefore of great interest to everyone.

The practice of wire drawing may be done using a single die or multiple dies (Figure 3) and involves pulling wire or rod through a die under cold working conditions in order to reduce the wire or rod to the desired shape and size. During its movement through the die, the wire passes through a very important part of the die known as the *deformation zone*. This is the working zone in which the diameter of the wire is reduced from an initial diameter (d_i) to a final diameter (d_f). Wire materials can be made from aluminium, copper, carbon steels, stainless steels or magnesium alloys while the working part of the die can be made out of natural or synthetic diamond and tungsten carbide (ASM International, 1988).

Multi-pass copper wire drawing normally proceeds in three stages: in the first stage (*rod breakdown*) an 8 mm rod is broken down to 4.00, 3.15 or 2.76 mm while in the second stage (*intermediate wire drawing*) the broken down copper wires are reduced to final copper conductor sizes ranging from 0.52 mm to 1.78 mm. Stage three (*fine wire drawing*) involves reduction of the intermediate wire to sizes ranging from 0.20 mm to 0.29 mm. The fine wire drawing produces mainly multi-stranded flexible cables.

Pass Schedule Designs

The shape of the deformation zone is greatly influenced by the process variables involved in wire drawing as shown in Figure 4. This zone exerts influence upon the redundant work, frictional work, and the total drawing forces during wire drawing (Hosford and Caddell, 1983).

The shape of the deformation zone exerts a strong influence on the properties and structure of wire material after drawing which include homogeneity of hardness, internal porosity, tendency to open cracks during processing and residual stresses (Hosford and Caddell, 1983).

The deformation zone is characterized by the delta parameter (Δ -parameter) which is a function of the area reduction, r , and the approach angle, α , and given by the following expressions (Wright, 2011):

$$r = \frac{A_i - A_f}{A_i} = 1 - \left(\frac{A_f}{A_i}\right) \quad [1]$$

$$\Delta \approx \left(\frac{\alpha}{r}\right) [1 + (1 - r)^{1/2}]^2 \approx 4 \frac{\tan \alpha}{\ln \left[\frac{1}{1-r}\right]} \quad [2]$$

Low Δ values are due to usage of small die angles and big reductions, while high Δ values indicate large die angles and low reductions (Wright, 2011). Whereas low Δ values indicate larger friction effects and surface heating due to longer wire contact in the approach zone, higher Δ values have a tendency toward void formation and centre bursting and are indicative of increased levels of redundant deformation and surface hardening due to excessive direction change during flow through the die. In many commercial operations, Δ values of 1.50 are likely to perform well during drawing operations whereas Δ values above 3.0 should generally be avoided (www.antaac.org).

Load-bearing capability of the wire can be expressed by the percent elongation ($E\%$). This concept is important especially considering wire breaks which are due to the necking and, thus, concentration of loads within the wire. The percent elongation during wire drawing is expressed by the following formular (Esteves Group, 2008):

$$E(\%) = \left[\left(\frac{d_i}{d_f}\right)^2 - 1 \right] \times 100 \quad [3]$$

The pass schedule concepts used in practical wire drawing include the following (Wright, 2011):

(i) *Constant area reduction*

Using this concept, a gauge system using the same area reduction and the approach angle for all passes is used. The advantage of this approach is that the emerging wire has a standard size meeting given specifications. Examples include the Brown and Sharpe (B&S) or American Wire Gauge (AWG).

(ii) *Constant Δ*

This approach is used when the area reduction varies yet there is a need to maintain a constant Δ value. The main motivation involves maintaining consistent values of die pressure, redundant work and centerline tension.

(iii) *Constant ratio of draw stress to yield stress*

Using this concept, the maximum area reduction in each pass can be obtained. This approach is a reflection of the work hardening that may take place as the wire passes through the die.

(iv) *Constant ratio of draw stress to average flow stress*

This concept is applied when the maximum area reduction in each pass is obtainable, while avoiding work hardening as the wire passes through the die.

Local Company Scenario

The facility layout commonly used in wire drawing plants is a typical *line or product layout*. This is so because such layouts produce relatively large quantities of a single item (Fogarty *et al.*, 1989). Figure 5 shows a typical industrial setup for intermediate wire drawing as practiced by one of the local firms in Zambia.

In the setup shown, copper rods of size 2.76 mm obtained from the rod breakdown machine are collected on a post (1). The copper wire (2) then passes through a take-up stand (3) towards the receiving blocks of the intermediate wire drawing machine (4). In the wire drawing machine, the copper wire is passed through die-sets (5) with dies of various sizes. Rotation of the capstans (6) within the wire drawing machine enables movement of the wire. The final copper wire is then passed through an annealer (7) and the tensioner (8) before being finally wound and collected on a drum (9).

Table 1 shows the pass schedules used to produce a 1.78 mm annealed copper wire. As seen from the table, the company's approach can be attributed to a constant Δ as the average value of Δ is 3.9.

Wire Damage Research

The geometry of the drawing die influences both the productivity and damage of the wire during its production (Bitkov, 2010). Wire damage may manifest in several forms such as damage due to cuts or abrasion, damage due to flow of the wire in the die and role of the lubricant and damage due to metallurgical or microstructural flaws (Wright, 2011).

Whereas all the three damage mechanisms are equally important, damage due to flow of wire in the die poses great challenges to the process engineer. This form of damage manifests as either central bursting or surface cracking. According to Avitzur (1983), central bursts (Figure 6) do not occur often but are important because they are internal and may cause unexpected failures in service, whereas surface defects (Figure 7) are as a result of the misalignment of the flowing wire or the generation of copper fines within the throat of the wire drawing die (Pops, 1997). Wright (2011) indicates that central bursting is as a result of the flow of the wire and the local stick-slip mechanism within the die passage.

Research done on central bursting during both wire drawing and extrusion processes by many researchers (Ahmadi and Farzin, 2008; Haddiet *al.*, 2012; Komori, 2003; Bitkov, 2010; Choi, et al., 2010; McAllen and Phelan, 2005) has affirmed the works of both Wright and Avitzur. Despite central bursting being common to both wire drawing and extrusion, the danger zone for wire drawing is much larger due to the fact that the average stress in extrusion is compressive while the same is tensile in wire drawing (Avitzur, 1983).

Research on ductile fracture and the mechanisms governing ductile damage under different fracture criteria has been done. Komori (1999) showed that the occurrence of central bursting is periodical and in the axial direction, while Hoffmann *et al.*(2000) showed that the occurrence of central bursting could be predicted using the flow stress and critical damage values. Ko and Kim (2000) and Reddy *et al.*(2000) showed that the fracture strain, the rate of nucleation and void growth under ductile fracture depended on the hydrostatic pressure around the central part of the deformed workpiece and the stress state outside this region.

Norasethasopon and Yoshida (2003) showed that the position, size and shape of inclusions and the number of drawing passes greatly influenced the formation of central bursting. McAllen and Phelan (2005, 2007) showed that the the effective strain and the die approach angle at different area reductions influenced central burst formation.

A modelling study and experimental investigation were undertaken to investigate the effects of the variation of the area reduction on internal and surface ductile damage of wrought copper wire under constant approach angle and friction conditions during multi-pass wire drawing. A combination of the ductile damage criterion and a Cockroft and Latham criterion was used to assess the initiation and progression of damage at different area reductions.

METHODOLOGY

Materials and Methods

Using atomic absorption spectrophotometry (AAS), chemical composition of the wrought copper rod material was obtained to ascertain levels of inclusions. A universal tensile testing machine was used to determine the engineering properties of the copper rod material and a scanning electron microscope was used to obtain internal and surface defect (void) micrographs. Abaqus 6.14 was used to model the wire drawing process.

Computational Conditions and Wire Drawing Modelling

Table 2 shows the pass schedules used to compute the modelling conditions based on the actual industrial setup shown in Figure 5 and using varying area reductions to obtain a final medium wire of diameter ranging from 1.68 to 1.78 mm.

Abaqus 6.14 Explicit environment was used to model the process using using a dynamic step, mass scaling and specifying a non-linear geometrical parameter in anticipation of large deformations. The scaling was applied to all regions of the copper wire with a target time increment of 0.00001, a linear bulk viscosity of 0.06 and a quadratic bulk viscosity of 1.2. The coulomb friction coefficient was kept constant at a value of 0.05. 4-node 2D axisymmetric quadrilateral elements, CAX4R, with reduced integration points and hourglass control, were used to mesh the deformable copper wire.

Using two analytically rigid dies with parameters $\alpha = 10^\circ$; $\gamma = 30^\circ$; $\beta = 40^\circ$; $L_b = 40\% d_f$, the copper wire drawing process was modelled as velocity-based with a drawing velocity of 0.08 m/s using four sequences of two-passes each. Table 3 shows the material properties used in the Abaqus models.

A centerline node 306 and a surface node 410, both located in a region of observed stress concentrations and opposite each other as shown in Figure 8 were selected. Stress and damage distributions for the nodes were then plotted and determined for the analysis.

Mathematical Models

The mathematical models for Mises equivalent stress (σ_{eq}), mean normal stress or hydrostatic pressure (σ_m), stress triaxiality (η) and the Cockroft and Latham criterion (C_{CL}) used are given by

the following expressions (Hosford and Caddell, 1983; Wright, 2011; Dassault Systèmes, 2013; Dassault Systèmes, 2014; Tan, 2009):

$$\sigma_{eq} = f(\sigma - \alpha) = \sqrt{\frac{3}{2}}(S - \alpha^{dev}) : (S - \alpha^{dev}) \quad [4]$$

where S is the deviatoric stress tensor ($S = \sigma + p\mathbf{I}$)

α^{dev} is the deviatoric part of the backstress tensor ($\alpha = \sigma - \sigma^0$)

$$\sigma_m = \frac{\sigma_{11} + \sigma_{22} + \sigma_{33}}{3} \quad [5]$$

where $\sigma_{11}, \sigma_{22}, \sigma_{33}$ are the radial, axial and circumferential stresses respectively.

$$\eta = -\frac{p}{\sigma_{eq}} \quad [6]$$

$$C_{CL} = \int_0^{\varepsilon^f} \sigma^* d\varepsilon_0 \quad [7]$$

Stiffness degradation formulation is based on a scalar damage approach involving a damage variable, D , (Dassault Systèmes, 2013):

$$\sigma = (1 - D)\sigma_e \quad [8]$$

The overall damage variable, D , captures all active damage mechanisms within the material. When the damage variable is equal to 1, a given material is understood to have completely failed.

RESULTS AND DISCUSSIONS

(1) Effects of Inclusions

The chemical composition of the copper wire shown in

Table 4 gives the levels of inclusions. Of particular interest are the levels of zinc which enters the copper as a solid solution and, up to 30 percent content, increases ductility in copper (John, 1992). The percentages of tin, manganese, iron and nickel in the copper are within the ASTM standard limits, avoiding possibilities of strengthening the copper matrix by possible dislocation mechanisms during wire entrance in the deformation zone. Due to the nature of the deformation

process, annealing of the copper wire is inevitable to avoid material strengthening through hardening, and hence crack formation.

(2) Effect of Area Reduction Variation on Mises Stress and Plastic Strain

Figure 9 (i) and (ii) shows that the von Mises stresses have values above the material yield stress and are tensile, in agreement with Avitzur (1983) that the average stress in wire drawing is tensile. The Mises stresses increase with area reduction for centerline nodes for all the multi-passes while for the surface nodes, Mises stresses tend to reduce slightly with increasing area reduction. Peaks are recorded at 16% area reduction during the second multi-pass for the centerline nodes, while surface nodes record a peak at 12% area reduction during the first multi-pass sequence.

Figure 9 (iii) and (iv) show that the plastic strain rises with area reduction for both nodes. For surface nodes, the plastic strain is higher during the first multi-pass stage while for centerline nodes the strain is independent of the multi-pass stages. Both nodes record a peak at 18% area reduction, supporting the works by McAllen and Phelan (2005, 2007) that the effective strain influences center bursting.

(3) Effect of Area Reduction Variation on Hydrostatic Pressure and Stress Triaxiality

Figure 10 (i) and (ii) show that the hydrostatic or mean stresses are compressive for the centerline nodes and tensile for the surface nodes. Peaks are recorded at 18% area reduction for all multi-passes, while the surface nodes record a peak at 12% area reduction during the second multi-pass sequence. The component axial stresses (σ_{22}) predominate and are compressive for centerline and tensile for surface nodes. The hoop stresses (σ_{33}) equally are compressive and tensile for centerline and surface nodes respectively. This agrees with Komori (1999) that the occurrence of central bursting is periodical and in the axial direction.

Figure 10 (iii) and (iv) shows that the stress triaxiality for the centerline nodes tends to increase as the area reduction increases, while for centerline nodes the stress triaxiality is stable except for the 16% area reduction point. Progressive damage and fracture under the Cockroft and Latham criterion normally occur under conditions of tensile hoop or circumferential stresses, or when stress triaxiality factors are greater than -0.333 (Bao and Wierzbicki, 2004). Hoop stresses are tensile for surface nodes and above -0.333 for centreline nodes, with peaks recorded during the first multi-pass stage. Cracking for both nodes is therefore likely to start from the first multi-pass stages, notable after 14% area reduction for centreline nodes.

(4) Effect of Area Reduction Variation on Damage Value and Cockroft and Latham Criterion

Figure 11 (i) and (ii) show that the damage value for both nodes increases with area reduction. The increase is set off from the 14% area reduction point for centerline nodes and accelerates, while for surface nodes damage sets in as early as the 12% area reduction point. Both nodes record peaks at 18% area reduction, with the first multi-pass recording highest damage values and the fourth multi-pass recording lower damage values.

Figure 11 (iii) and (iv) show that the Cockroft and Latham criterion has a similar behaviour to damage value distribution, though with the opposite multi-pass stages. The Cockroft and Latham criterion is reached during the fourth multi-pass sequence at 16% area reduction for centerline nodes and just above the 14% area reduction mark for surface nodes during the third multi-pass stage. Peaks are recorded at 18% during the third multi-pass for centerline nodes and during the second, third and fourth multi-pass stages for surface nodes.

Since damage during wire drawing is cumulative and can be assessed with the Cockroft and Latham criterion (Wright, 2011), it was observed from the models that the damage for ductile criterion, D , reached the limiting value of 1 at 16% area reduction for centerline nodes and during all the area reduction variations for surface nodes. Being a fundamental index of workability and drawability, the Cockroft and Latham criterion is highly influenced by the levels of plastic strain (Wright, 2011). Figure 9 (iii) and (iv) show that strain is highest at higher area reductions, with the first multi-pass sequence recording higher values for surface nodes.

The micrographs in **Error! Reference source not found.** and **Error! Reference source not found.** show damage initiation during the first and fourth multi-pass stages. The damage distributions in Figure 11 (i) and (ii) are therefore understood to reflect the absolute extent of damage initiation for each node at every multi-pass, whereas the Cockroft and Latham distributions in Figure 11 (iii) and (iv) show the cumulative extent which is a progression of the damage. The defect micrographs show that for centreline nodes, damage is possible with area reductions of 16% and above, whereas for surface nodes damage is possible even at 10% area reduction with the first multi-pass stage impacting greater damage.

(5) Effect of Area Reduction Variation on Elongation and Δ -Parameter

Figure 14 shows that at constant approach angles, an increase in area reduction leads to increased elongation but reduced delta values. Further reduction in delta values imply higher area reductions with accelerated strain and consequent damage values. Under such cases, the elongation is quite high and the stress triaxiality very high. Though commercially recommended, delta values less than 3.00 require a good balance of other impacting factors as the wire is highly prone to damage

due to high strains and damage value indices. This is because damage initiation is inevitable as seen from the damage models, hence the progression of damage is what needs to be controlled.

CONCLUSIONS

From the models and study of defect micrographs, the following conclusions can be drawn:

(1) Pure copper contains impurities which act as inclusions within the copper matrix. Metallurgical control of the levels of these inclusions is mandatory before the copper is further drawn to reduce on the possibilities of the inclusions being centres of cracking due to stress concentration.

(2) Damage initiation during copper wire drawing starts with the first multi-pass stage. Progression of damage will depend on the area reduction and the corresponding plastic strain attained. Damage progression will occur at 12 and 16% area reductions during the fourth multi-pass stages for the surface and centerline nodes respectively. Damage, thus will initiate and progress earlier for surface nodes, and later for centerline nodes.

(3) Damage progression is independent of the multi-pass schedule for centerline nodes, but highly dependent on multi-pass stages for surface nodes.

(4) Wire breakages attributed to small delta values, large area reductions are mainly due to increased stress triaxiality and elongation, thus encouraging necking of the wire. Wire drawing practitioners need a good balance of parameters when operating with small delta values and high area reductions.

(5) Due to strict productivity requirements when operating at high area reductions and low delta values, wire drawing practitioners should ensure conditions within the deformation zone remain as prescribed as possible. This is typical when drawing fine wires. Usage of robust die nib materials such as natural or polycrystalline diamond become necessary in order to avoid early wear of the approach zone and movement to a higher delta zone.

(6) The local micro and small-scale wire practitioners need a good understanding and application of the drawing die material and pass schedule design techniques. A 'floating' pass schedule, using area reduction, delta parameter and ratio of flow to yield stress is encouraged due to limitations with equipment for ensuring constancy of conditions in the deformation zone.

Due to the interaction and complexity of variables at play during copper wire drawing, a good selection of variables and constant monitoring of the process is inevitable during wire drawing

practice. Apart from a good pass schedule design which is very important, conditions such as lubrication, temperatures in the die-wire zone and drawing speed need to be monitored.

ACKNOWLEDGEMENTS

The authors would like to thank the National Science and Technology Council (NSTC) under the Zambian Ministry of Education, Science, Vocational Training and Early Education for material and financial support towards this research study.

REFERENCES

- [1] Ahmadi, F. and M.Farzin, M. (2008). Investigating Geometric and Friction Conditions Causing Chevron Cracks in Wire Drawing Process using FEM. *Steel Research International Journal: Special Edition Metal Forming* , 2, 382 -388.
- [2] Antaac.org. (n.d.). *Theory of Wire Drawing*. [Online]
<http://www.antaac.org.mx/descargas/TheoryOfWiredrawing.pdf>. Retrieved 24-03-2012.
- [3] ASM Handbook, (1988), Volume 14: Forming and Forging, ASM International.
- [4] Avitzur, B. (1983). *Handbook of Metal-Forming Processes*. John Wiley and Sons, Inc.
- [5] Bao, Y. and Wierzbicki, T. (2004). A Comparative Study on Various Ductile Crack Formation Criteria . *Transactions of the ASME* , 126, 314-324.
- [6] Bitkov, V. (2010). Minimisation of Breaks during Drawing Thin Wire of Non-Ferrous Metals. *Russian Journal of Non-Ferrous Metals* , 51 (2), 134-139.
- [7] Dassault Systèmes. (2014). Abaqus Analysis Users Guide.
- [8] Dassault Systèmes. (2013). *Modelling Fracture and Failure with Abaqus*.
- [9] Esteves Group. (2008). *The e-Wizard: Your Wire Die Handbook*. Retrieved from http://www.estevesgroup.com/ewizard/esteves_ewizard_en/

- [10] Fogarty, D., Hoffman, T., and Stonebraker, P. (1989). *Production and operations management*. Cincinnati: South Western Publishing Co.
- [11] Haddi, A., Imad, A. and Vega, G. (2012). The Influence of the Drawing Parameters and Temperature Rise on the Prediction of Chevron Crack Formation in Wire Drawing. *International Journal of Fracture* , 176, 171-180.
- [12] Hoffmann, J., Vazquez, V., Vega, C., and Altan, T. (2000). Prediction of Ductile Fracture in Forward Extrusion with Spherical Dies. *Transactions of NAMRI/SME* , 28, 57-62.
- [13] Hosford, W. and Caddell, R. (1983). *Metal Forming: Mechanics and Metallurgy*. Prentice Hall.
- [14] International Copper Study Group. (2016). *World Copper Fact Book 2016*. Lisbon: International Copper Study Group.
- [15] John, V. (1992). *Introduction to Engineering Materials* (Third ed.). Basingstoke: Macmillan.
- [16] Kalpakjian, S. and Schmid, S. (2006). *Manufacturing Engineering and Technology* (5th ed.). Pearson.
- [17] Kalpakjian, S. and Schmid, S. (2010). *Manufacturing Engineering Technology*. Pearson.
- [18] Ko, D.-C. and Kim, B.-M. (2000). The Prediction of Central Burst Defects in Extrusion and Wire Drawing. *Journal of Materials Processing Technology* , 102, 19-24.
- [19] Komori, K. (2003). Effect of Ductile Fracture Criteria on Chevron Crack Formation and Evolution in Drawing . *International Journal of Mechanical Sciences* , 45, 141-160.
- [20] Komori, K. (1999). Simulation of Chevron Crack Formation and Evolution in Drawing. *International Journal of Mechanical Sciences* , 41, 1499-1513.
- [21] McAllen, P. and Phelan, P. (2005). A Method for the Prediction of Ductile Fracture by Central Bursts in Axisymmetric Extrusion. *Proceedings of the Institution of Mechanical Engineers, Part C: Journal of Mechanical Engineering Science* , 237-250.
- [22] McAllen, P. and Phelan, P. (2007). Numerical Analysis of Axisymmetric Wire Drawing by Means of a Coupled Damage Model. *Journal of Materials Processing Technology* , 183, 210-218.

- [23] Norasethasopon, S. and Yoshida, K. (2003). Influence of an Inclusion on Multi-Pass Copper Shaped-Wire Drawing by 2D Finite Element Analysis. *IJE Transactions B: Applications*, 16 (3), 279-292.
- [24] Pops, H. (1997). The Metallurgy of Copper Wire. Copper Development Association Inc.
- [25] Reddy, N., Dixit, P. and Lal, G. (2000). Ductile Fracture Criteria and its Prediction in Axisymmetric Drawing. *International Journal of Machine Tools and Manufacture*, 40, 95-111.
- [26] Tan, H. (2009). *Flow Theory of Plasticity*. Retrieved 02 12, 2016, from <http://homepages.abdn.ac.uk/h.tan/pages/teaching/plasticity/Flow.pdf>
- [27] Wright, R. (2011). *Wire Technology: Process Engineering and Metallurgy*. Butterworth-Heinemann.

TABLES AND FIGURES

Table 1 Pass Schedule Design for Producing a 1.78 mm Copper Wire

Pass No	d_i (mm)	d_f (mm)	r (%)	Δ	Pass No	d_i (mm)	d_f (mm)	r (%)	Δ
1	2.76	2.55	14.6	4.0	4	2.11	1.92	17.2	3.7
2	2.55	2.32	17.2	3.7	5	1.92	1.78	14.1	4.2
3	2.32	2.11	17.3	3.7					

Table 2 Drawing Pass Schedules under Different Area Reductions

	Pass No	d_i (mm)	d_f (mm)	Pass No	d_i (mm)	d_f (mm)
$r = 10\%$; $\Delta = 6.69\%$; $E=11.11\%$	1	2.76	2.62	6	2.12	2.01
	2	2.62	2.48	7	2.01	1.91
	3	2.48	2.36	8	1.91	1.81
	4	2.36	2.24	9	1.81	1.72
	5	2.24	2.12			
	1	2.76	2.59	5	2.14	2.01

$r = 12\%$; $\Delta = 5.52$; $E=13.64\%$	2	2.59	2.43	6	2.01	1.88
	3	2.43	2.28	7	1.88	1.76
	4	2.28	2.14			
$r = 14\%$; $\Delta = 4.68$; $E=16.28\%$	1	2.76	2.56	4	2.20	2.04
	2	2.56	2.37	5	2.04	1.89
	3	2.37	2.20	6	1.89	1.76
$r = 16\%$; $\Delta = 4.04$; $E=19.05\%$	1	2.76	2.53	4	2.12	1.95
	2	2.53	2.32	5	1.95	1.78
	3	2.32	2.12			
$r = 18\%$; $\Delta = 3.55$; $E=21.95\%$	1	2.76	2.49	4	2.05	1.86
	2	2.49	2.26	5	1.86	1.68
	3	2.26	2.05			

Table 3 Material Parameters used during Modelling

Parameter			Parameter		
Symbol	Description	Value	Symbol	Description	Value
E	Youngs Modulus	118.75 GPa	α	Approach angle	0.15707 radians
σ_y	Yield stress	165.738 MPa	ρ	Density	8960 kgm ⁻³
ν	Poisson's ratio	0.34	ϵ_{fr}	Fracture strain	0.338
η	Stress triaxiality	-1.72	$\dot{\epsilon}$	Strain rate	0.0015s ⁻¹
C_{CLCRT}	Critical C_{CL} Damage criterion	357.99 MPa	μ	Coefficient of friction	0.05

Table 4 Chemical Composition of Wrought Copper

Constituent Elements (norm. wt %)									
Sb	As	Cd	Fe	Pb	Mn	Ni	Ag	Zn	Cu
<0.04	<0.01	<0.002	0.12	<0.01	0.002	0.003	<0.01	0.04	Bal.

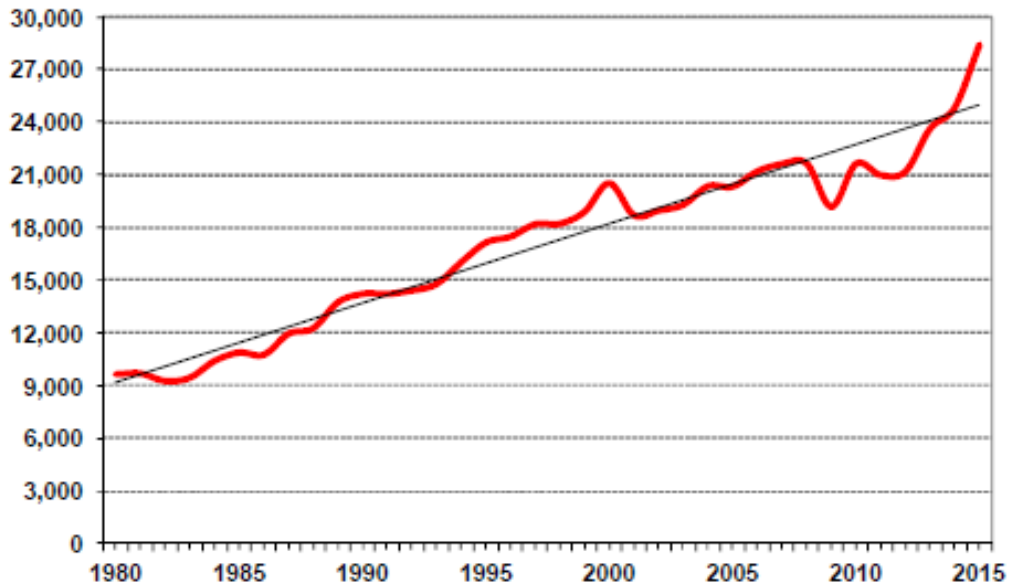


Figure 1 World Copper and Copper Alloy Semis Production in thousand metric tonnes
Source: (International Copper Study Group, 2016)

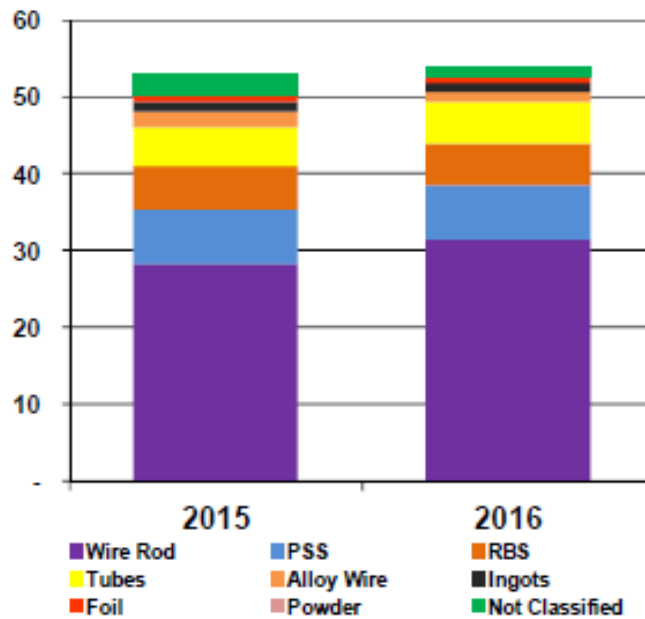


Figure 2 Copper Semis Production in million tonnes gross weight
Source: (International Copper Study Group, 2016)

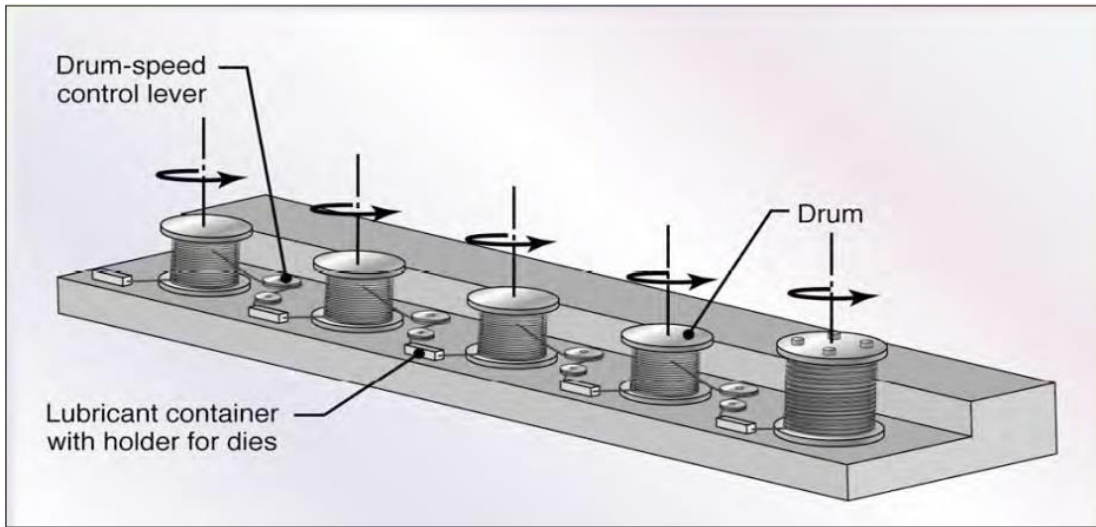


Figure 3 Multiple Wire Drawing Machine Source: (Kalpakjian and Schmid, 2006)

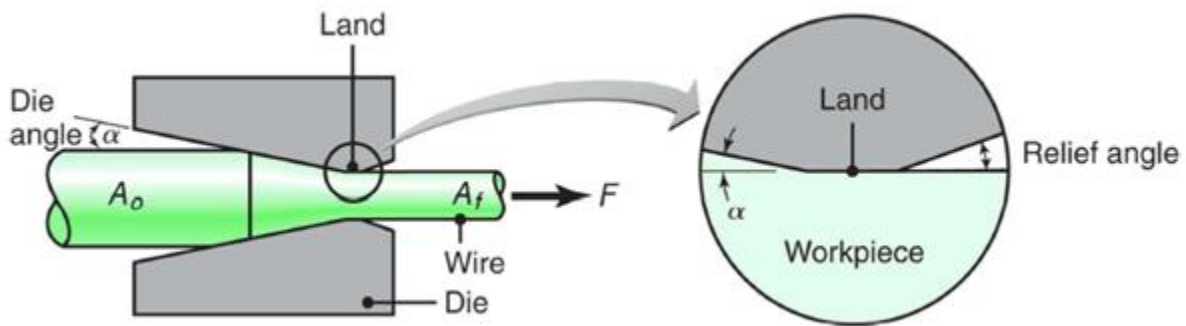


Figure 4 Process Variables in Wire Drawing

(Source: Kalpakjian and Schmid, 2010)

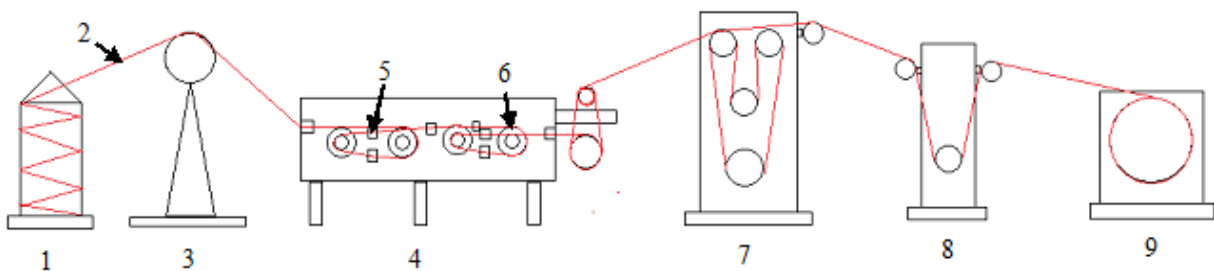


Figure 5 Schematic Plant Layout of a Multi-Pass Copper Wire Drawing



Figure 6 Wire Break due to Centre Burst Source: (Wright, 2011)

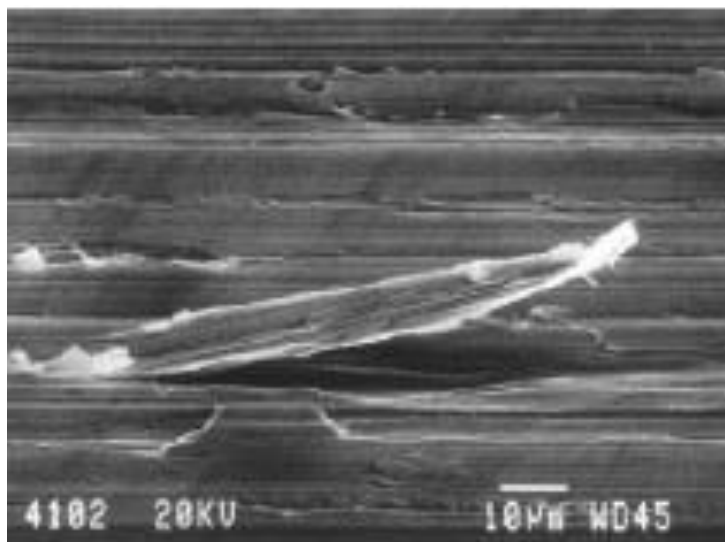


Figure 7 Fines on Copper Wire Surface Source: (Wright, 2011)

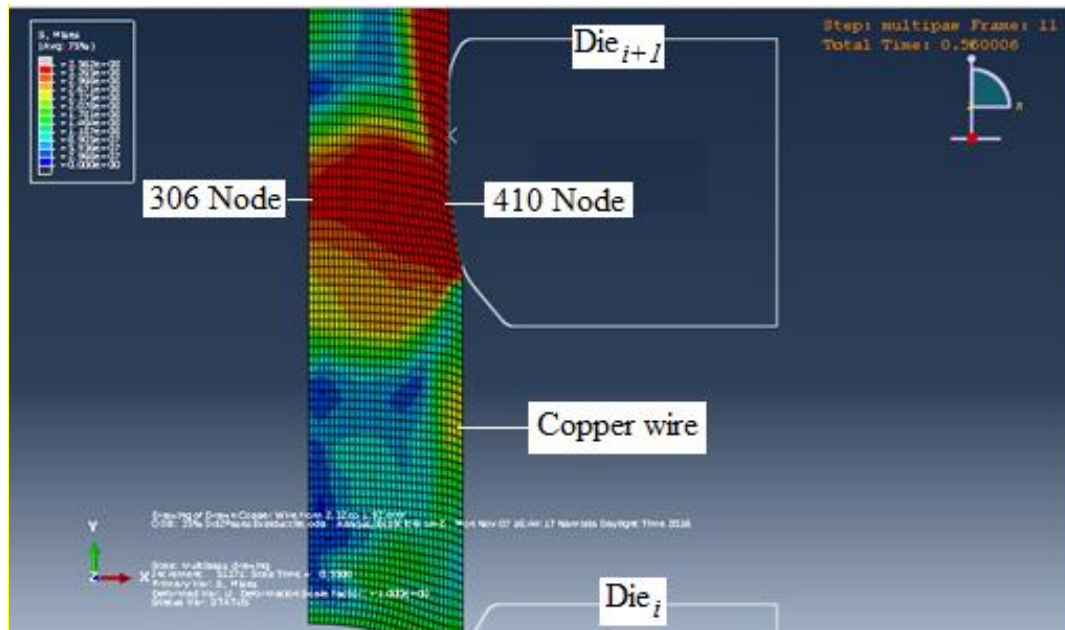


Figure 8 2D Axisymmetric Modelling of Multi-Pass Copper Wire Drawing

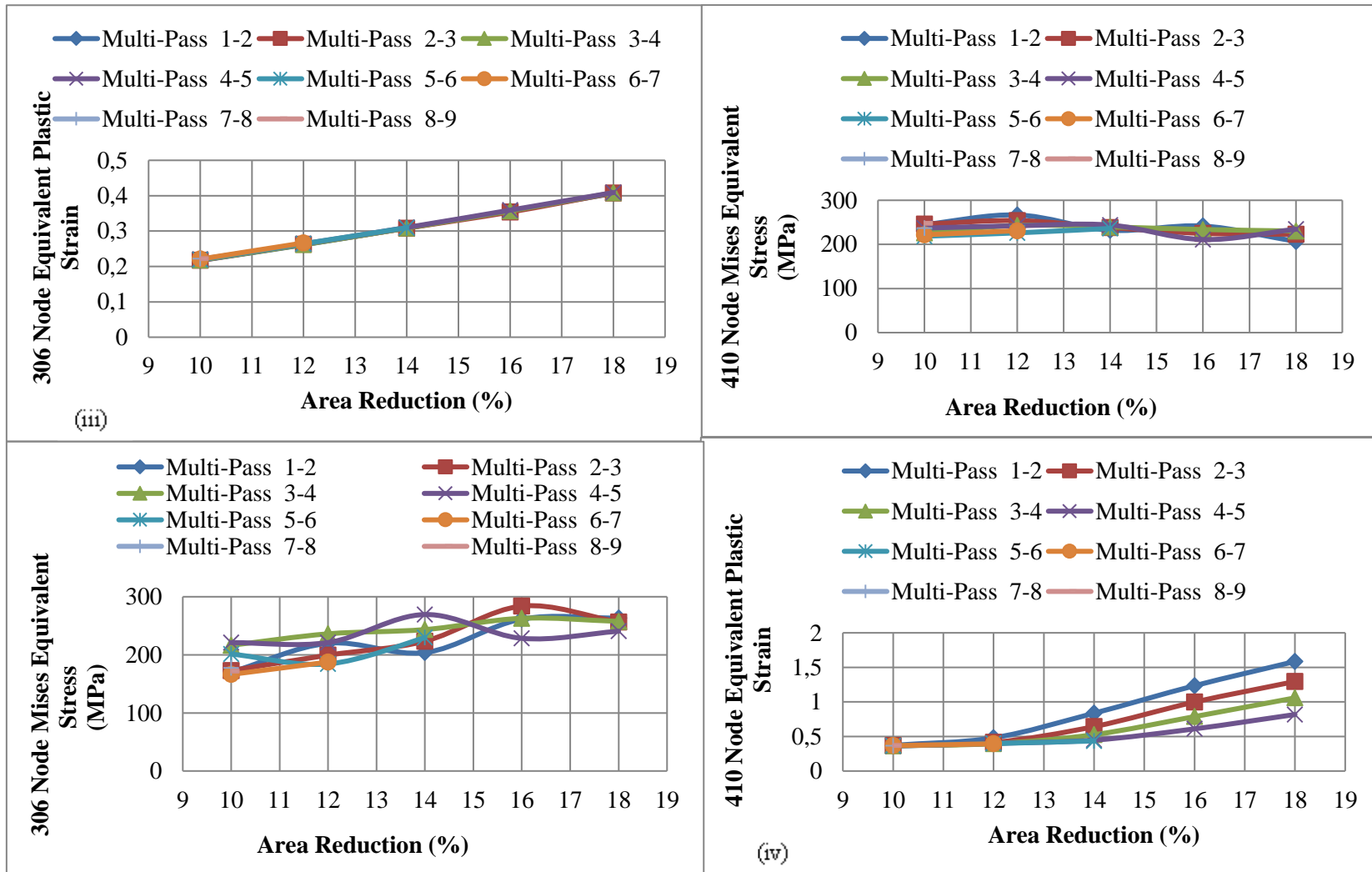


Figure 9 Variation of Equivalent Mises Stress and Plastic Strain with Area Reduction

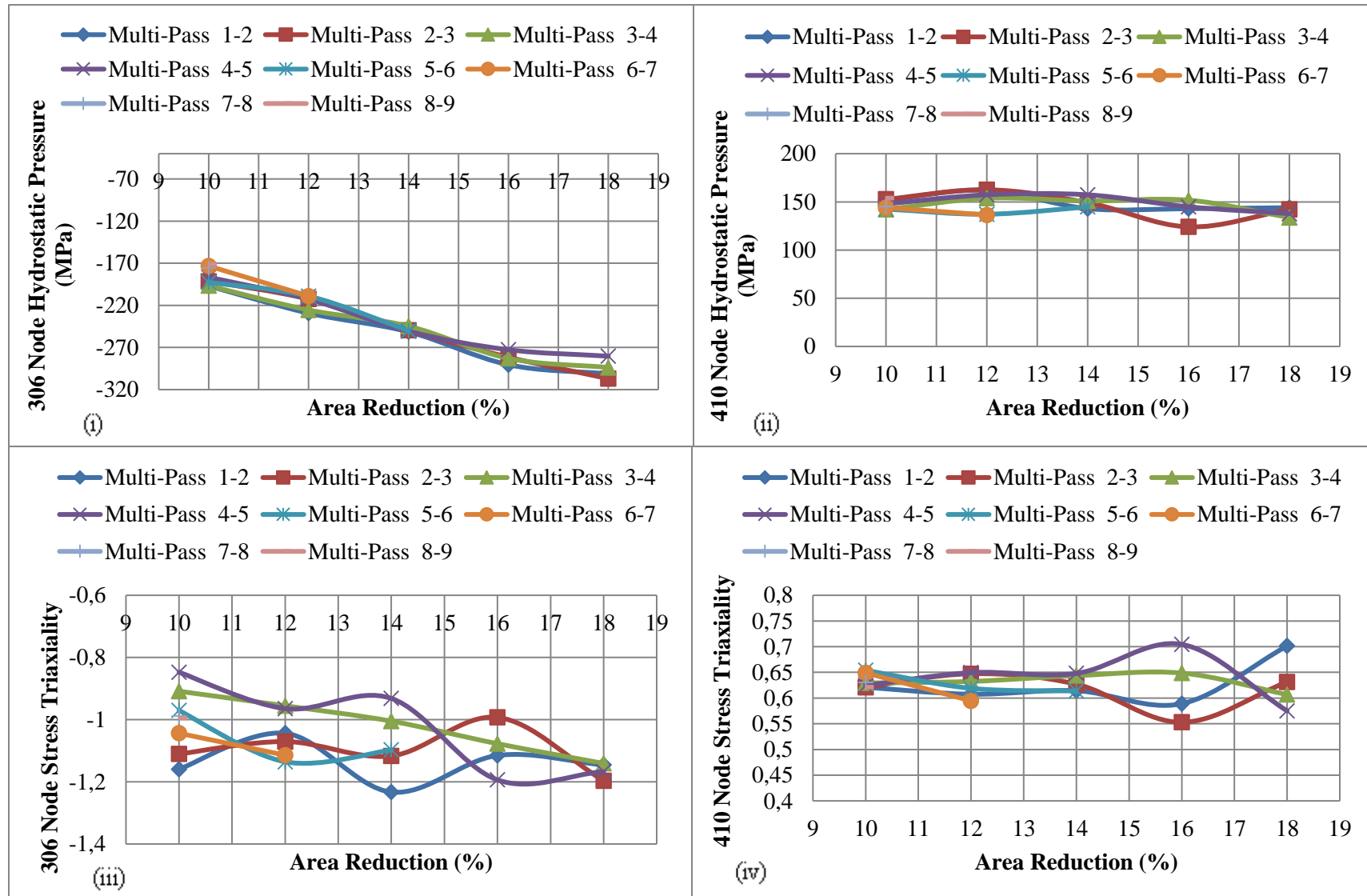


Figure 10 Variation of Hydrostatic Pressure and Stress Triaxiality with Area Reduction

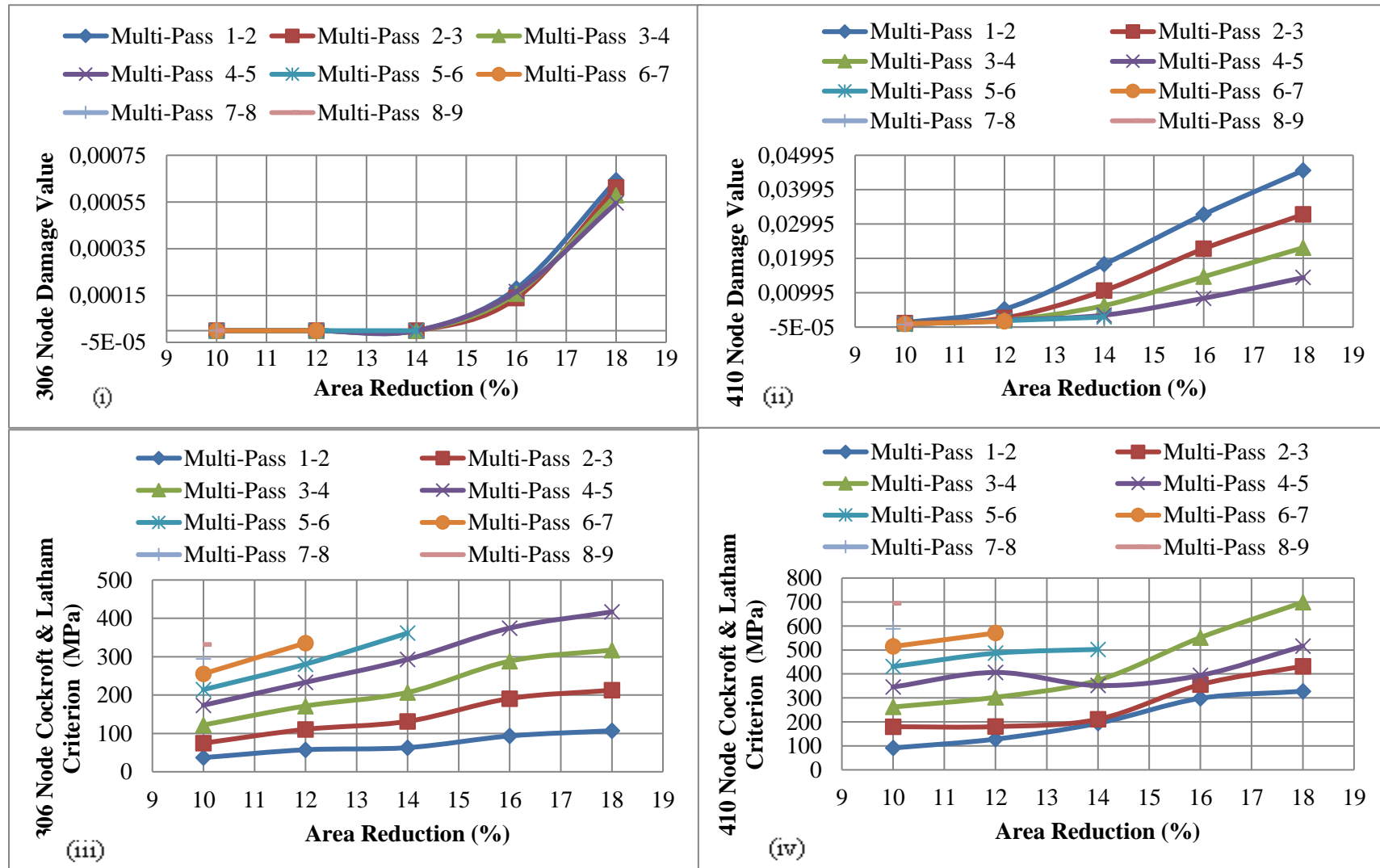


Figure 11 Variation of Damage Value and Cockroft and Latham

Criterion with Area Reduction

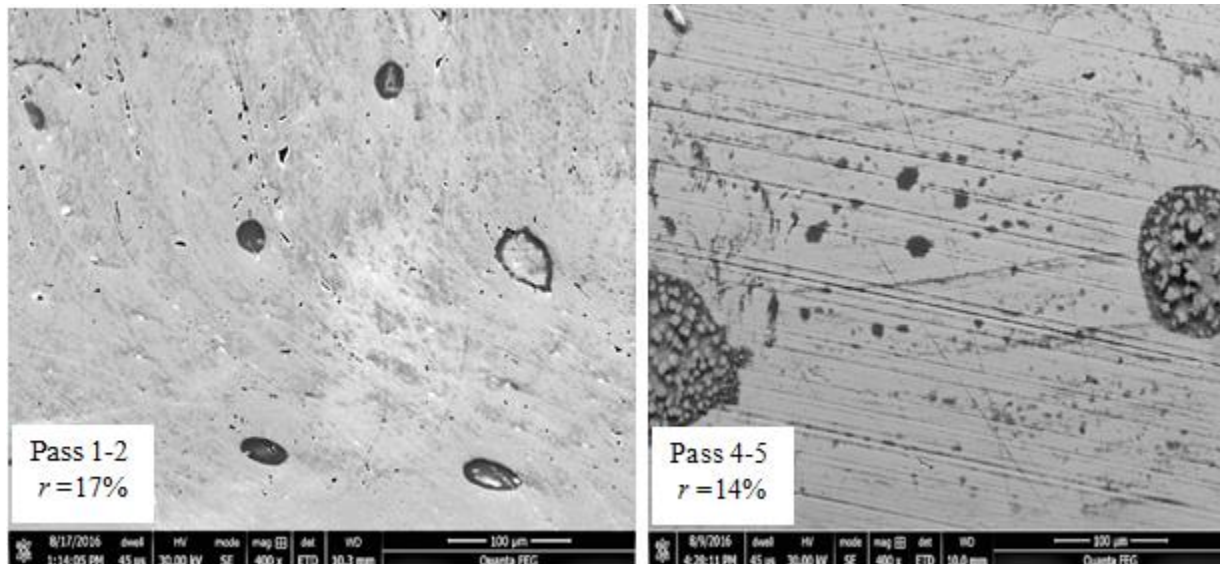


Figure 12 Micrographs of Internal Void Formation during First and Fourth Multi-Pass Stages

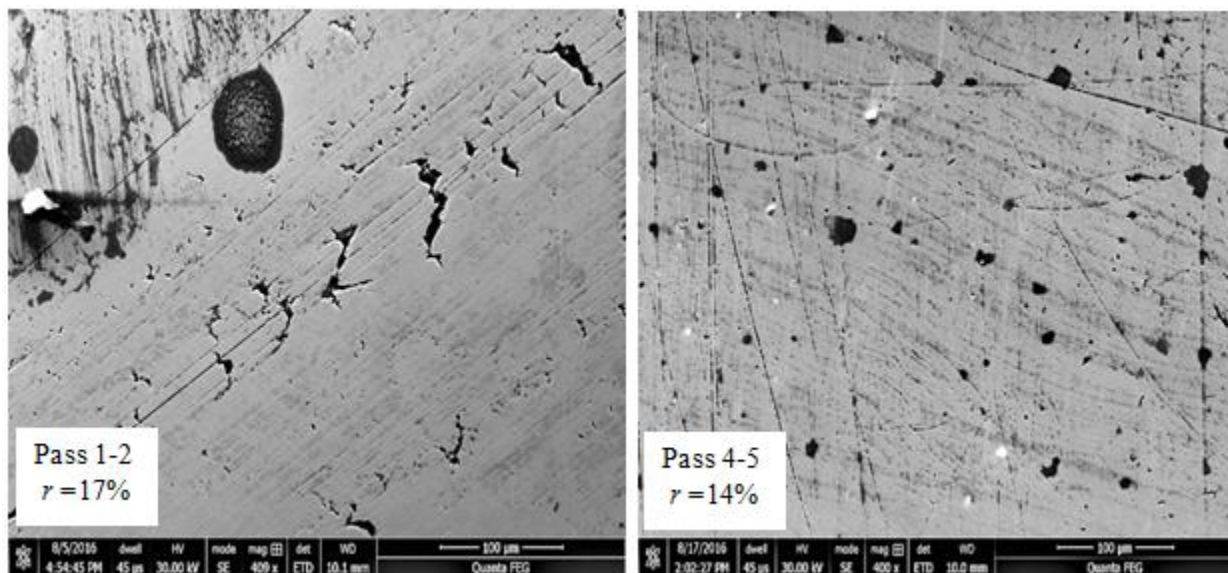


Figure 13 Micrographs of Surface Defects during Third and Fourth Multi-Pass Stages

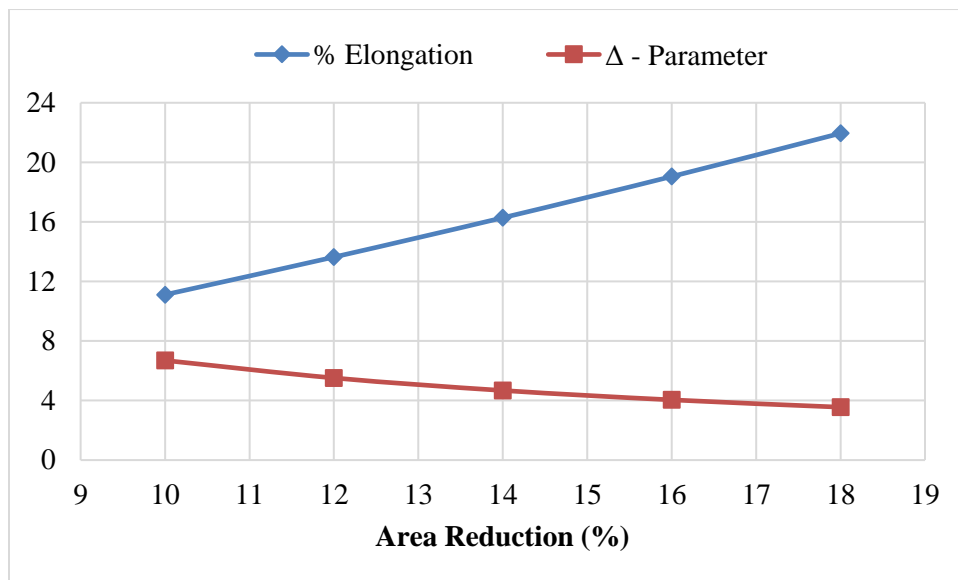


Figure 14 Variation of Elongation and Δ parameter with Area Reduction